



Removing Eddy-Current probe wobble noise from steam generator tubes testing using Wavelet Transform

L.A.N.M. Lopez ^{a,*}, D.K.S. Ting ^b, B.R. Upadhyaya ^c

^a The University Center of FEI, Mechanical Engineering Department, São Paulo, Brazil

^b Nuclear Engineering Center, Nuclear and Energetic Research Institute, São Paulo, Brazil

^c Nuclear Engineering Department, University of Tennessee, Knoxville, USA

Abstract

One of the most important nondestructive evaluation (*NDE*) applied to steam generator tubes inspection is the electromagnetic Eddy-Current testing (*ECT*). The signals generated in this *NDE*, in general, contain many noises which make difficult the interpretation and analysis of *ECT* signals. One of the noises present in the signals is the probe wobble noise, which is caused by the existing slack between the probe and the tube walls. In this work, Wavelet Transform (*WT*) is used in the probe wobble de-noising. *WT* is a relatively recent mathematical tool, which allows local analysis of non-stationary signals such as *ECT* signals. This is a great advantage of *WT* when compared with other analysis tools such as Fourier Transform. However, using *WT* involves wavelets and coefficients' selection as well as choosing the number of decomposition level needed.

This work presents a probe wobble de-noising method when used in conjunction with the traditional *ECT* evaluation. Comparative results using several *WT* applied to Eddy-Current signals are presented in a reliable way, in other words, without loss of inherent defect information.

A stainless steel tube, with two artificial defects generated by electro-erosion, was inspected by a *ZETEC MIZ-17ET ECT* equipment. The signals were de-noised through several different *WT* and the results are presented. The method offers good results and is a promising method because it allows for the removal of Eddy-Current signals' probe wobble effect without loss of essential signal information.

© 2007 Elsevier Ltd. All rights reserved.

Keywords: Eddy-Current; Probe wobble; Noise; Steam generator; Wavelet Transform

1. Introduction

Steam generators tubes' bundles can be inspected by several different types of nondestructive evaluation (*NDE*).

The most common *NDEs* are Visual Inspection, Ultra-Sound and Eddy-Current testing (*ECT*). For in situ inspection, due to lay out restrictions as well as operational conditions, Eddy-Current testing (*ECT*) is one of the best choices applicable to steam generators' defect detection. Classification and localization of the defect by the *ECT* inspection allow for corrective actions to be taken in due time in order to assure reliable and safe operation of the steam generator (Stegemann et al., 1997).

ECT is an electromagnetic test whose signals are presented in the impedance (*Z*) plane as "8" shaped Lissajous figures (Stegemann, 1986). Those figures are formed when bobbin coil probes passes through the internal side of inspected tubes. Fig. 1 presents the Lissajous figure formation.

ECT signals have resistive (*R*) and inductive (X_L) components in such a way that:

$$\vec{Z} = \vec{X}_L + \vec{R} \quad (1)$$

or,

$$|Z| = \sqrt{X_L^2 + R^2} \quad (2)$$

The Lissajous figure is formed as the impedance values change in the impedance plane as presented in Fig. 2.

* Corresponding author. Tel.: +55 11 43532900x2172; fax: +55 11 41095994.

E-mail address: luizlopez@fei.edu.br (L.A.N.M. Lopez).

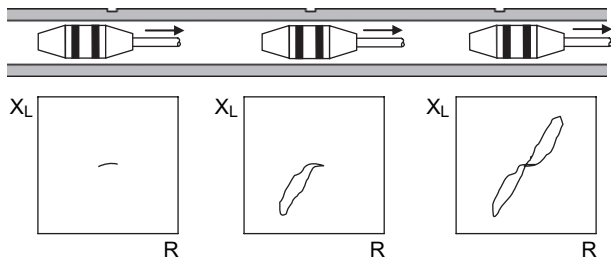


Fig. 1. Lissajous figure formation.

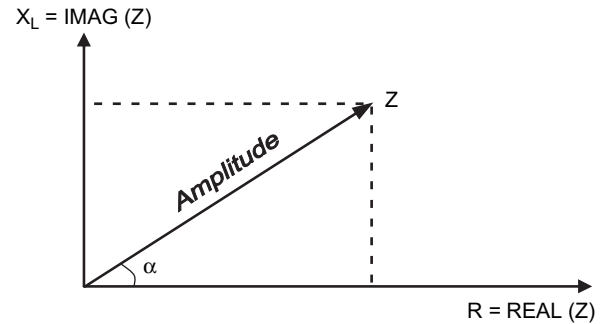


Fig. 2. Impedance plane.

Fig. 3 presents a typical standard noise free *ECT* signal in the impedance plane and its resistive and inductive components.

However, when the signal is contaminated by noises, the interpretation of the *ECT* signals is done subjectively by the inspectors which can induce, for the sake of conservatism, to premature closure of tubes. The unnecessary plugging of tubes reduces capability of heat transmission and can result in equipment scrapping. On the other hand, if a damaged tube is not plugged, it can fail during operation causing leakage and obvious losses.

The noises present in *ECT* signals frequently change strongly the shape of the Lissajous figures. To avoid such a situation, the lesser amount of noise in the signal, the interpretation of the signal will be more precise, the lesser the chances of an incorrect decision being taken.

The most common noises are caused by signal acquisition interference (Lopez et al., 2003), material magnetic characteristics (Lopez et al., 2005) and probe fluctuation (lift-off effect) (Lopez and Mazaro, 2003). Fig. 4 shows an extremely noisy *ECT* signal.

One of the most common noise, which is always present, is due to the probe wobble inside the tube caused by the needed gap between the probe and the inner wall (Stegemann, 1986). The probe wobble produces a low frequency fluctuation in the signal, which changes the voltage amplitudes of the reactive component jeopardizing the correct localization and dimensioning of a defect. In this work, we use the Discrete Wavelet Transform (*DWT*) (Chui, 1992) as an alternative to the traditional phase discrimination method (Stegemann, 1990). *DWT*

removes efficiently the noise caused by the probe fluctuation without losing original information contained in the signal, about the defect being sought.

A *DWT* applied to signal processing is a relatively new technique and allows for localized time frequency analysis of non-stationary signals such as the *ECT* signals. This is the greatest advantage of *DWT* when compared to other analysis tools such as the Fourier Transform, for example, which relies on the periodicity of the function to obtain an acceptable result. *DWT* is sensible to discontinuities in the time domain, which is an important characteristic of *ECT* signals. Using *DWT* requires, however, the correct choice of the wavelet functions $\psi_{j,k}(t)$ and the selection of the transformed coefficients $C(j,k)$ at a given scale decomposition level.

The objective of this work is to present *DWT*, as a fundamental tool to remove the noise generated by *ECT* probe wobble, and to show the effects of using different wavelet functions.

The signals processed in this present work were generated by an *ZETEC MIZ-17ET ECT* inspection equipment, as presented in Fig. 5, using probes with circumferential bobbin coils in a differential mode arrangement.

The *ECT* signals were acquired using *LABVIEW* software and the signals were processed through an algorithm (Lopez et al., 2006; Lopez, 2002) specially conceived in *MATLAB* software.

Only the inductive voltage components, X_L of the inspection coil circuit, were considered in this work. The voltage

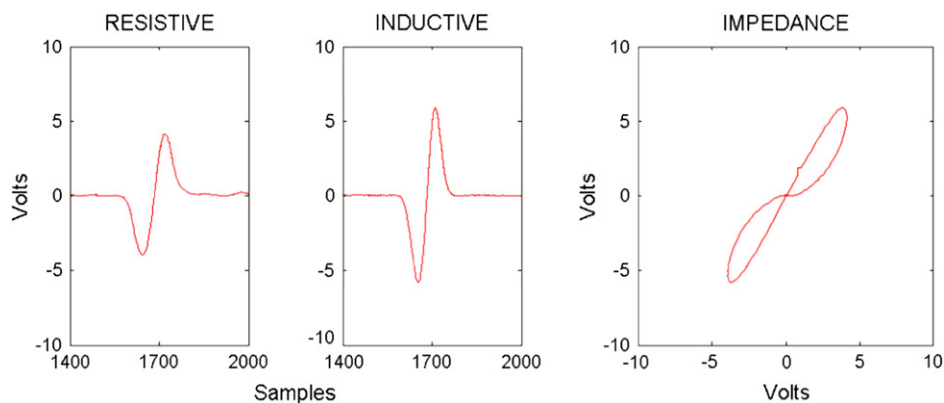


Fig. 3. Resistive, inductive and impedance plan views.

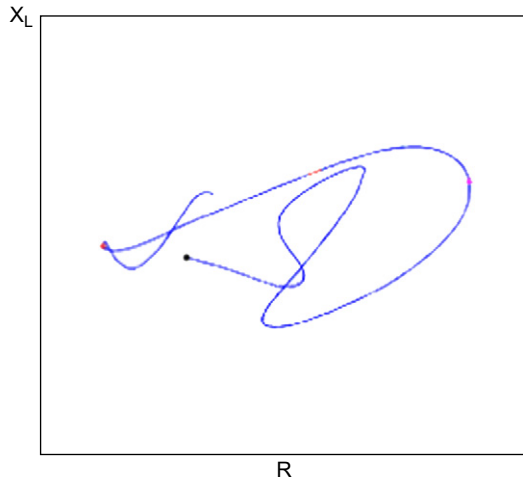


Fig. 4. Effect of noise in ECT signal.

changes in the signal are caused by discontinuities found by the probe, which change the material properties, in particular the electrical conductivity σ .

The inspections were carried out on a stainless steel tube *ASTM-A-249-316L*, 19.05 mm inside diameter, 1.24 mm wall thickness (*BWG 18*), with two artificially implanted defects produced by electro-erosion, in the form of full through wall holes with 0.9 mm and 1.1 mm in diameter, properly separated from each other, as presented in Fig. 6.

2. The Discrete Wavelet Transform (DWT)

The *DWT* of a given signal $s(t)$ is the family of coefficients $C(a,b)$, which depends on the two index a and b . Viewed from an intuitive standpoint, the wavelet decomposition can be considered as the calculation of “similarity indices” between the signal and the wavelet function at each time shift b and scale a . If the index has a high value, the similarity is high and otherwise, it is weak. These indices are named the coefficients $C(a,b)$ and are defined by Eq. (3).

$$C(a,b) = \int_R s(t) \frac{1}{\sqrt{a}} \psi\left(\frac{t-b}{a}\right) dt \quad (3)$$

where

$$a = 2^j, \quad b = k2^j, \quad (j,k) \in \mathbb{Z}^2 \quad (4)$$

Substituting a and b in Eq. (3) results:

$$C(j,k) = \int_R s(t) 2^{-(j/2)} \psi(2^{-j}t - k) dt \quad (5)$$

The *DWT* of $s(t)$ is defined as the signal projection in a set of wavelet functions $\psi_{j,k}(t)$,

$$\text{DWT}(j,k) = \int_R s(t) \psi_{j,k}(t) dt \quad (6)$$

where

$$\psi_{j,k}(t) = 2^{-(j/2)} \psi(2^{-j}t - k) \quad (7)$$

To be efficient and useful, an analysis method should be capable of performing the signal synthesis and the *WT* has this capability.

The analysis starts by decomposing and transforming the signal at each scale level resulting in the coefficients $C(j,k)$. The synthesis starts from the coefficients $C(j,k)$ and reconstructs the original signal $s(t)$ by inverse transforming. For finite energy signals the wavelet inverse transform is defined by Eq. (8):

$$s(t) = \sum_{j \in \mathbb{Z}} \sum_{k \in \mathbb{Z}} C(j,k) \psi_{j,k}(t) \quad (8)$$

From the synthesis equation, one can obtain the approximations and details of the original signal at each level j by summing over every time shift k , from Eq. (8), which is shown in Eq. (9) for the detail part of the decomposed signal:

$$D_j(t) = \sum_{k \in \mathbb{Z}} C(j,k) \psi_{j,k}(t) \quad (9)$$

Performing now the summing over all levels j , one can recover the original signal using all the details as shown in Eq. (10):

$$s(t) = \sum_{j \in \mathbb{Z}} D_j \quad (10)$$

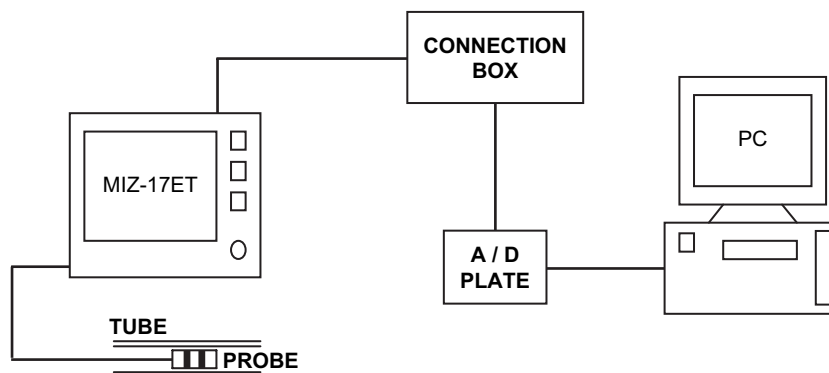


Fig. 5. MIZ-17ET ECT equipment and hardware scheme.

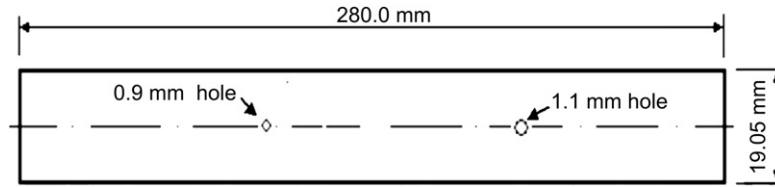


Fig. 6. ASTM-A-249-316L tube.

All the details are therefore considered. Defining a reference detail level J , one can separate two classes of details. Those with level $j \leq J$ corresponding to scales $a = 2^j \leq 2^J$ which can be called refined details. And the others with $a = j > J$ are the coarse details. These details are grouped according to Eq. (11):

$$A_J = \sum_{j>J} D_j \quad (11)$$

and named it as approximations to the signal $s(t)$, which can be calculated by Eq. (12):

$$s(t) = A_J + \sum_{j \leq J} D_j \quad (12)$$

Eq. (12) can be written as:

$$s(t) = D_1 + D_2 + \dots + D_j + \dots + A_J \quad (13)$$

where

$$j = 1, 2, \dots, J \quad (14)$$

The approximation A_J at a given level j is the high scale component at that level containing the low frequency information. On the other hand, the detail D_j is the low scale component with the high frequency content. Each approximation A_J is decomposed in another approximation and detail. For j level decompositions, there exists $j + 1$ possible decompositions for a given signal. Fig. 7 shows, as an example, the decomposition tree of a signal to $j = 3$:

$$s(t) = A_3 + D_3 + D_2 + D_1 = A_2 + D_2 + D_1 = A_1 + D_1 \quad (15)$$

The decomposition presented by Eq. (15) allows us to separate the noise from the useful part of the signal. Additionally, the useful part of the signal can be extracted by using the coefficients already calculated from the decomposition.

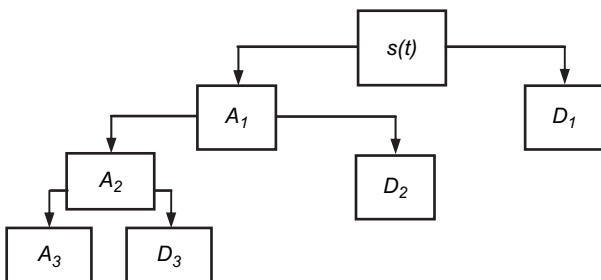


Fig. 7. Multiple level WT decomposition tree.

3. Wavelet Transform used to noise removal

The probe wobble noise removal was studied by using four selected wavelets: Haar, Biorthogonal, Biorthogonal Reverse and Daubechies (Daubechies, 1992).

3.1. The Haar Wavelet

The Haar Wavelet $\psi_{\text{Ha}}(x)$ is the simplest possible wavelet. It is the first known wavelet and was proposed in 1909 by Alfred Haar. This wavelet is a step function and therefore is not differentiable, which represents a disadvantage. The values assumed by this wavelet are:

$$\psi_{\text{Ha}}(x) = 1 \text{ to } x \in [0, 0.5] \quad (16)$$

$$\psi_{\text{Ha}}(x) = 0 \text{ to } x \in [0, 1] \quad (17)$$

$$\psi_{\text{Ha}}(x) = -1 \text{ to } x \in [0.5, 1] \quad (18)$$

Fig. 8 presents the Haar Wavelet function.

3.2. The Daubechies Wavelets

The Daubechies Wavelets' family $\psi_{\text{Db}N}(x)$ is composed of nine members, from Db2 to Db10, as presented in Fig. 9.

The Daubechies Wavelet was invented by Ingrid Daubechies, one of the most brilliant researcher in the world of wavelets. The Daubechies Wavelets $\psi_{\text{Db}N}(x)$, where N is the order, are compactly supported orthonormal wavelets defining a DWT. These wavelets are in general not symmetric and some present a very pronounced asymmetry. They have no explicit expression, except for $N = 1$, which is the same as Haar Wavelet:

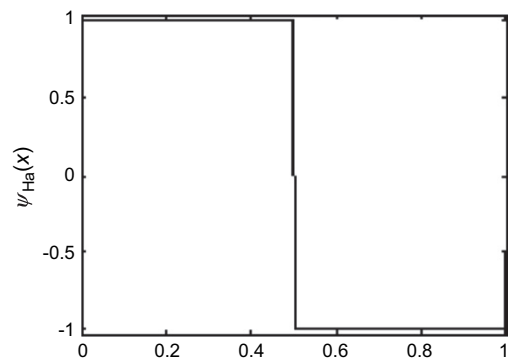


Fig. 8. The Haar Wavelet.

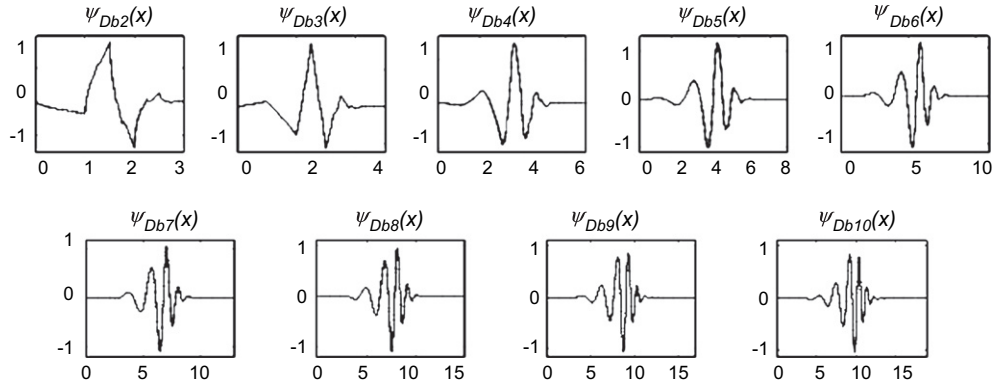


Fig. 9. The Daubechies Wavelet family.

$$\psi_{Db1}(x) = \psi_{Ha}(x) \quad (19)$$

In this work, Daubechies 5 Wavelet was selected after some testing due to its great compatibility with the resistive and inductive components of *ECT* signals.

3.3. Biorthogonal and Biorthogonal Reverse Wavelets

The Biorthogonal Wavelet family uses in fact two wavelets, one for decomposition and the other for reconstruction, instead of the same one like Daubechies transform. This characteristic results in the property of linear phase, which is necessary for *ECT* signals reconstruction. The decomposition or analysis wavelet generates the coefficients of a signal $s(x)$:

$$\tilde{C}_{(j,k)} = \int_R s(x) \tilde{\psi}_{j,k}(x) dx \quad (20)$$

The wavelet $\psi_{j,k}$ is then used in the reconstruction or synthesis process:

$$s = \sum_{j,k} \tilde{C}_{j,k} \psi_{j,k} \quad (21)$$

The wavelets ψ and $\tilde{\psi}$, that can have very different regularity properties, are related by duality as follows:

$$\int \tilde{\psi}_{j,k}(x) \psi_{j',k'}(x) dx = 0 \quad (22)$$

as long as $j \neq j'$ or $k \neq k'$ and even,

$$\int \tilde{\phi}_{O,k}(x) \phi_{O',k'}(x) dx = 0 \quad (23)$$

as long as $k \neq k'$

In addition, the functions ψ , $\tilde{\psi}$, ϕ and $\tilde{\phi}$ assume zero values outside of a segment. Fig. 10 shows the decomposition wavelet function ϕ and the corresponding recomposition wavelet function ψ of four Biorthogonal Wavelet functions. In this work were used the wavelets Biorthogonal 3.5 and Biorthogonal Reverse 3.5.

The Biorthogonal Reverse family is obtained from the Biorthogonal Wavelet family above described.

The wavelet selection took in to account the visible differences among some wavelets. The four selected wavelets are presented in Fig. 11 for comparison.

These wavelets were used to processing signals generated in the inspection of the stainless steel tube presented in Fig. 6.

The number of decomposition levels affects the signal processing (Mallat, 1989). In this article is presented the result of several wavelet application to the signal decomposed in nine levels, allowing the appropriate selection of D_j and A_j coefficients.

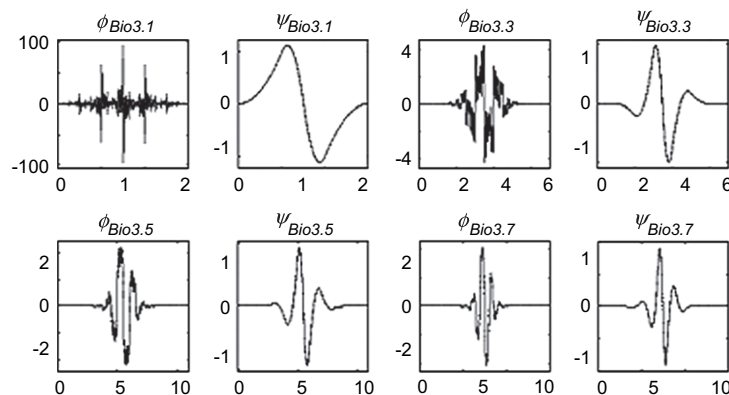


Fig. 10. Four wavelets from the Biorthogonal family.

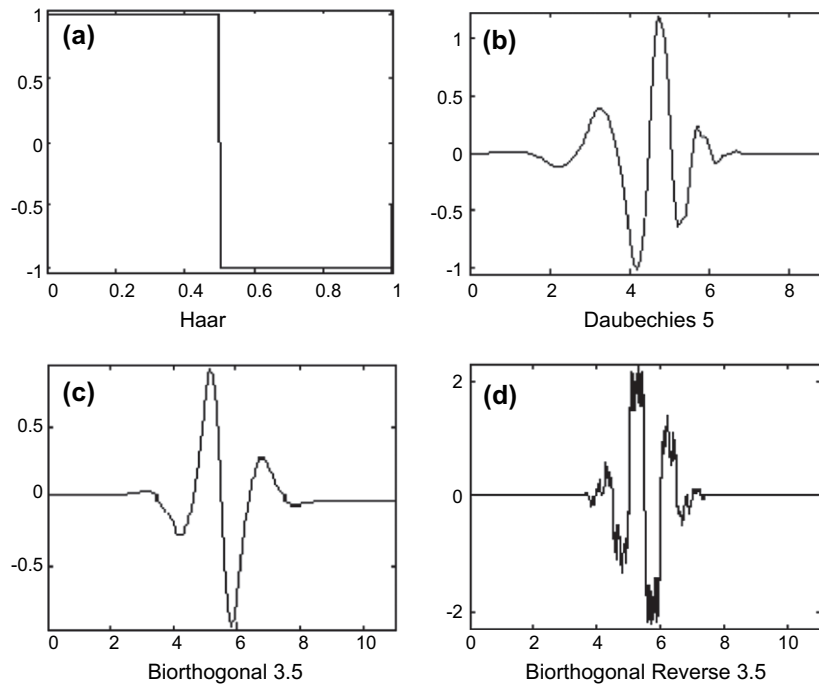


Fig. 11. Wavelets selected to process the signal.

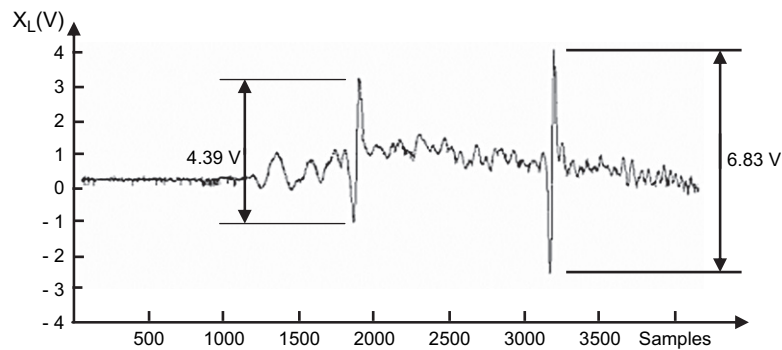
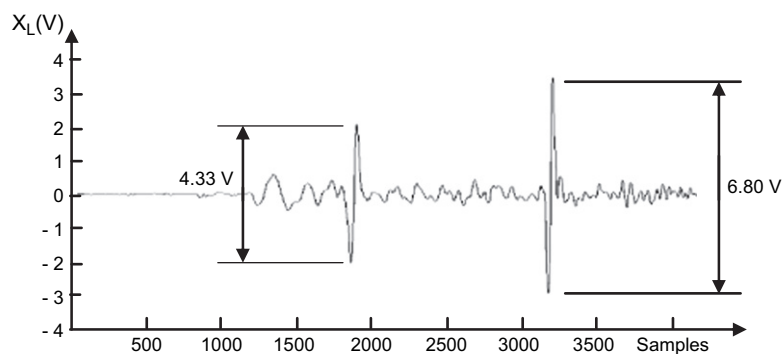
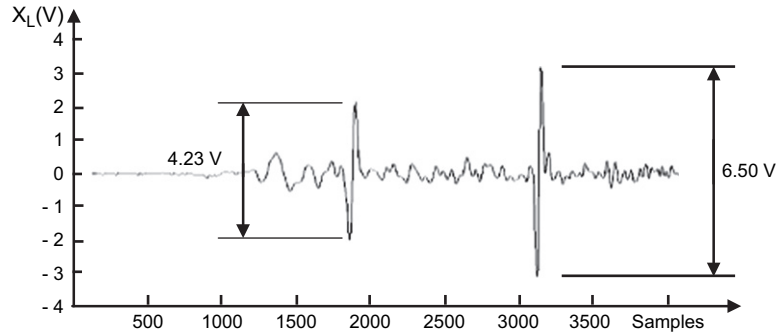
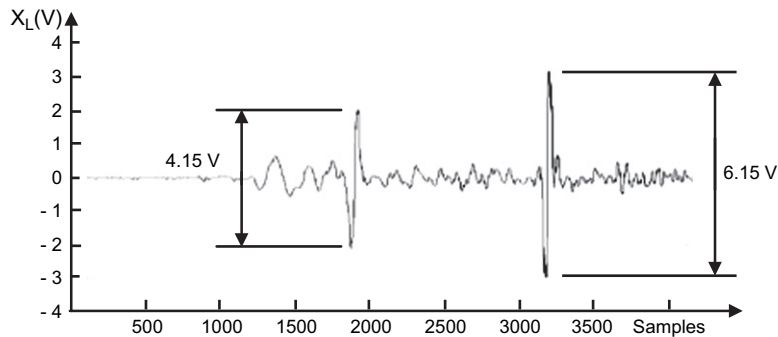
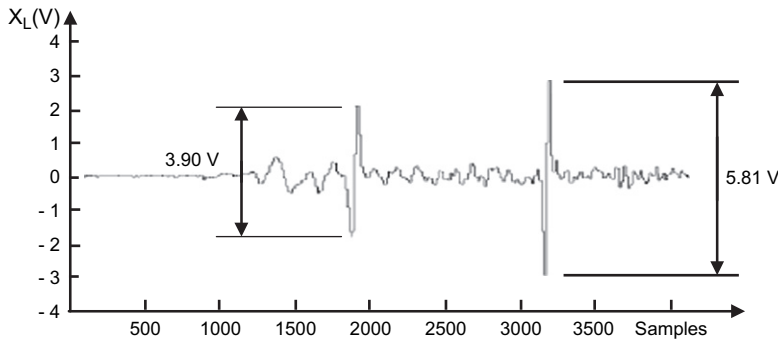


Fig. 12. Original signal.

Fig. 13. Processed signal through *DWT* Daubechies 5.

Fig. 14. Processed signal through *DWT* Biorthogonal 3.5.Fig. 15. Processed signal through *DWT* Biorthogonal Reverse 3.5.Fig. 16. Processed signal through *DWT* Haar.

4. Experimental results and discussion

The four wavelets presented above were used to process the original noisy signal presented in Fig. 12. This signal is the inductive component (X_L) of the Lissajous figure obtained from passing the probe through the inspected tube inner side. It is a usual procedure the use of the *ECT* signal inductive component in the analysis process made by Eddy-Current inspectors.

Figs. 13–16 present, respectively, the results of *DWT* application through the use of wavelets Daubechies 5, Biorthogonal

3.5, Biorthogonal Reverse 3.5 and Haar to the original signal, removing A_J approximation which is the low frequency and high amplitude signal component.

The most important result that can be observed is the original signal lower frequency components' removal.

Fig. 12 shows that there is a low frequency component in the signal with amplitudes which can reach 1 V in a region where the signal should be around 0 V. The low frequency component is completely eliminated through all processes.

The criterion that distinguishes the efficiency of a wavelet application is that it should keep the signal total amplitude

unchanged because this parameter is extensively used by Eddy-Current inspectors. Fig. 13, which shows the use of the Daubechies 5 *DWT*, presents the best result by noting that the signal amplitude was approximately unchanged.

Figs. 14 and 15 show the results of using Biorthogonal 3.5 and Biorthogonal Reverse 3.5 *DWTs*. The signal amplitude limits were reduced from 4.39 V to 4.23 V and 4.15 V in the first defect and from 6.83 V to 6.50 V and 6.15 V in the second defect, respectively. This is a reduction which can jeopardize the inspector decisions with respect to defect characterization.

The results presented in Fig. 16, where it used a Haar *DWT*, can be considered unacceptable under Eddy-Current inspection point of view because it presents big amplitude reductions. It is important to note that all figures present a remaining noise due to tube imperfections and that was not removed because it is not a consequence of probe wobble inside the tube.

5. Conclusion

From the above comparison, it can be concluded that Daubechies 5 *DWT* presents the best results due to the non-symmetric shape of its wavelet function, which is best adjustable to the transient nature of Eddy-Current signal. This wavelet removes efficiently the noise due to probe wobble without signal characteristics' changes, allowing the use of the *DWT* as an alternative to the traditional phase discrimination method.

The results presented through Biorthogonal Reverse 3.5 *DWT* use are worst than those presented through Biorthogonal 3.5 *DWT* because wavelet function peaks are not compatible with Eddy-Current signal peaks. The Haar *DWT* use not only changed hardly the signal reactance limits as well as its resolution, because besides being symmetric, it also presents a discontinuity.

Acknowledgements

The authors wish to thank to O.P. Negrão Jr. (Interativa – Manutenção Preditiva Ltd.), for his collaboration.

References

- Chui, C.K., 1992. An Introduction to Wavelets. Academic Press, London.
- Daubechies, I., 1992. Ten Lectures on Wavelets. CBMS-NSF Regional Conference Series in Applied Mathematics, Philadelphia, Pennsylvania.
- Lopez, L.A.N.M., 2002. Wavelet Transform and Fuzzy Logic in the Eddy-current Inspection of Nuclear Power Plants Steam Generator Tubes. PhD thesis, Universidade de São Paulo.
- Lopez, L.A.N.M., Ting, D.K.S., Upadhyaya, B.R., 2003. Application of wavelet transform in de-noising eddy current testing signals of heat exchanger tubes. In: 17th International Congress of Mechanical Engineering – COBEM 2003, São Paulo.
- Lopez, L.A.N.M., Ting, D.K.S., Upadhyaya, B.R., 2005. Removing material noise in eddy-current inspections of steam generators tubes using wavelet transform. In: 18th International Congress of Mechanical Engineering – COBEM 2005, Ouro Preto.
- Lopez, L.A.N.M., Mazaro, C.F., 2003. Remoção do Efeito Lift-Off de Sinais de Eddy-current por meio de Transformadas de Wavelets. In: Third Pan American Conference on NDT – 3rd PANNDT, Rio de Janeiro.
- Lopez, L.A.N.M., Ting, D.K.S., Upadhyaya, B.R., 2006. Automatic detection and sizing of eddy-current testing Lissajous figures. In: Conferência Internacional sobre Evaluación de Integridad y Extensión de Vida em Equipos Industriales – IEV 2006, São Paulo.
- Mallat, S., July 1989. A theory for multiresolution signal decomposition: the wavelet representation. IEEE Transactions on Pattern Analysis and Machine Intelligence 11 (7), 674–693.
- Stegemann, D., 1986. Avanços Tecnológicos em END por Correntes Parasitas. Revista dos END ABENDE, 23–29.
- Stegemann, D., 1990. Fundamentos do Método de Correntes Parasitas. International Cooperation, ABENDE, 132 pp.
- Stegemann, D., Reimche, W., Feiste, K.L., Heutling, B., 1997. Characterization of Materials Behavior by Electromagnetic Nondestructive Testing. MARCON, Knoxville, Tennessee, pp. 87.01–87.09.